JOURNAL OF MATERIALS SCIENCE 22 (1987) 4476–4483

The use of a ring tensile test to evaluate plasma-deposited metals

R. L. MEHAN, M. R. JACKSON, J. R. RAIRDEN, W. T. CARTER
General Electric Research and Development Center, General Electric Company, Schenectady 12301, New York, USA

A ring tensile test using a split disc fixture was developed and used to evaluate the tensile properties of a low-pressure plasma-deposited nickel-base superalloy from 25 to 1010° C. These properties were compared to those obtained with conventional uniaxial tensile specimens. It was concluded that the ring tensile test is an adequate test to rapidly and inexpensively evaluate the strength of thin (~1.0 mm) as-deposited plasma-deposited structures. A finite-element analysis of the test indicated that for sufficiently large deformation (~2%) the stress and strain fields approximated those of a uniaxial distribution.

1. Introduction

Arc-plasma spraying has been used for over 30 years to deposit coatings for various applications [1]. These coatings are typically 80 to 90% dense and have oxygen contents greater than 2000 p.p.m. Low-pressure plasma deposition (LPPD) has been developed during the past 15 years to apply high-density coatings with a low oxygen content [2]. More recently, the same process has been used to produce free-standing structural components [3]. The advantages of the LPPD process to produce structural members have been previously described [3, 4]. In brief, compositional flexibility can be achieved in complex shapes in near-final form, and composite structures consisting of either continuous or discontinuous laminates can be produced [5]. These laminated structures can range from those containing ductile–ductile constituents to ductile–brittle, with the brittle phase being a ceramic. Generally, the LPPD process is particularly well suited for producing thin-walled components in order to minimize costly machining operations.

As with all metallurgical processes, LPPD-produced structures must be evaluated with respect to their physical and mechanical properties. These properties are needed for process control and for design purposes; ideally, the same evaluation method will serve both needs. Generally, tensile tests are made on round or flat specimens; from these data the fundamental properties of elastic modulus, strength and ductility are obtained. The same (or very similar) specimen geometry can be used to evaluate the other properties of prime concern for high-performance structural members such as rupture and fatigue strength.

While it is possible to deposit thick layers of material by LPPD processing from which test specimens can be machined, it is much easier and less costly to produce near-net shapes consisting of thin-walled structures (of the order of 1.0 mm) similar to those that are needed for components such as aircraft vanes and combustor cans. Therefore, it would be highly advantageous to test specimens machined from a simple thin-walled tubular structure. This approach would have the added advantage that the same metallurgical structure would be present in the test specimen as in the engineering component.

The purpose of this paper to describe such a test: a ring tensile test on thin-walled structures that provides for a rapid and low-cost evaluation of LPPD materials and yields information applicable to engineering needs such as strength and ductility. Details of the test will be described, and a comparison will be made between the ring tensile and conventional tensile properties for the nickel-based superalloy IN-100. Based on this comparison, and an analytic evaluation of the ring tensile test, the applicability of the ring tensile test in evaluating LPPD structures will be assessed.

2. Background of the ring tensile test

The ring tensile test, also referred to as the split-D and NOL (Naval Ordnance Laboratory) ring tensile test, has been used for many years to evaluate filament-wound composites [6, 7]. It is an ASTM test [8] for evaluating tubular plastics, and because of the ease of manufacturing the specimen and conducting the test it remains a popular evaluation technique in spite of its obvious drawback; the non-uniform stress distribution.

In its original form, the test consists of inserting split- D-shaped fixtures into a ring with an inside diameter of 146 mm, an outside diameter of 147.51 mm and a width of 6.35 mm [8]. The ring and aligned D fixtures are placed in a tensile machine and pulled apart. Because of the conformity of the fixtures with the ring, an average internal pressure loading is achieved. The load–elongation curve from the test is used to compute tensile properties.

This test has been criticized by Dow *et al.* [9], who found the bending stress was sufficiently high to raise questions about the engineering merit of the tensile strength values measured as the P/A stress at maximum load in the ring. These authors proposed a "racetrack" specimen, which has two straight sections

0022–2461/87 $03.00 + .12

adjacent to the split in the D fixtures. Another suggestion proposed to alleviate the bending problems involves internal pressurization of the ring [6]. These modifications, while all useful in obtaining a more uniaxial stress state, add to the complexity of the test, the simplicity of which is one of its most attractive features. This was recognized by Knight [7], who analysed the ring tensile test as applied to advanced composite materials by a combination of finite-stress analysis and Weibull statistical strength theory. With such an analysis, Knight concluded that the ring tensile test is "an adequate and reasonably accurate method" as applied to advanced filamentary composites with Weibull moduli $\lesssim 40$. He points out, however, that rings thicker than the standard ASTM dimensions (ring radius/wall thickness < 50) may give results with significant errors. Very similar results have been reported by Vemura and Mirrata [10], who also show the advantage of the "racetrack" specimen.

The use of ring tensile tests to evaluate metallic materials, composites or otherwise, is not nearly as widespread as for filamentary wound polymeric composites. Krashchenko and Gurarii [11] have presented a review of work conducted in the USSR using this technique. They also draw attention to the same shortcoming of the test (non-uniform stress distribution), but do indicate satisfactory agreement between strength values determined using ring tensile and conventional tensile bars. Similarly, Kolesnichenko and Yusupov [12] have reported satisfactory results for ring specimens of Al–B fibre-reinforced composites. Apart from these authors, very little reported work seems to be available for metallic materials on the relationship of ring tensile properties and conventional tensile tests, particularly as a function of temperature.

It may be noted that the somewhat related problem of combined tension and bending in the plastic range which is present at the location where the split-D fixtures meet has been studied by Frankland and Roads [13]. In their analysis and testing programme conducted on an aluminium alloy, only the comparison of pure bending and bending in the presence of tensile stresses was discussed. The authors conclude, not surprisingly, that the strength under combined tension and bending is greatly affected at low levels of ductility, while the strength is substantially independent of combined stress of ductility at high values of ductility. These results, although interesting, are difficult to apply to the ring case as used for high-strength nickel-based alloys. What is significant is that low values of ductility will reduce the ring strength compared to the tensile strength, but a numerical value for "low" ductility is uncertain.

3. Experimental and analytical procedure

3.1. The LPPD process

Deposits were produced in the following manner to allow comparison of the ring and bar tensile tests. Mandrels of steel tube 3.8 cm in diameter and 10 cm in length were placed in a low-pressure plasma deposition chamber and the chamber was evacuated to < 2 torr. An Ar–He plasma was initiated and brought to steady-state operation at 80 kW. At the same time, the vacuum pumps were throttled to achieve a steady-state chamber pressure of 60 torr. With the steel mandrel rotating about the long axis of the tube, the tube was translated back and forth under the plasma at a rate of approximately 12 cm sec^{-1}. This was continued until the tube temperature approached a near-equilibrium value, approximately 1000° C for the gun-to-substrate distance used. Then powders of -325 mesh size ($< 44\,\mu m$) were injected at two opposite points, transverse to the plasma, at a rate of 9 kg h^{-1} to produce cylinders of either 1.1 or 6.3 mm in wall thickness. These deposits were approximately 97% of the theoretical density of the alloy. The deposits were heat-treated on the mandrel at 1250° C for 2 h in argon, and then cooled rapidly in argon. This heat treatment produces grain sizes of $\sim 25\,\mu m$ in most γ'-strengthened superalloys. Densification of internal (closed) porosity occurs during this heat treatment, and measured densities are usually 100% of theoretical density. There generally is some surface connected porosity in the outer 75 to 100 μm of the deposit. Fig. 1 shows representative micrographs of ring and bar specimens removed from each deposit. As may be seen, the deposition procedure in both cases produced an equiaxed grain structure with a slightly larger grain size for the thin deposition.

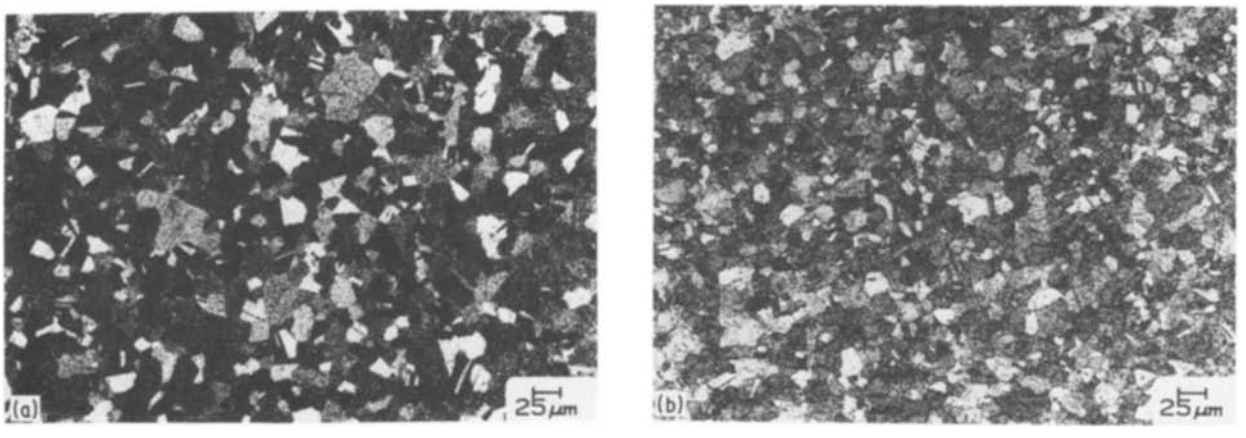

Figure 1 Photomicrographs of LPPD IN-100: (a) thin deposit (ring specimen), (b) thick deposit (bar specimen).

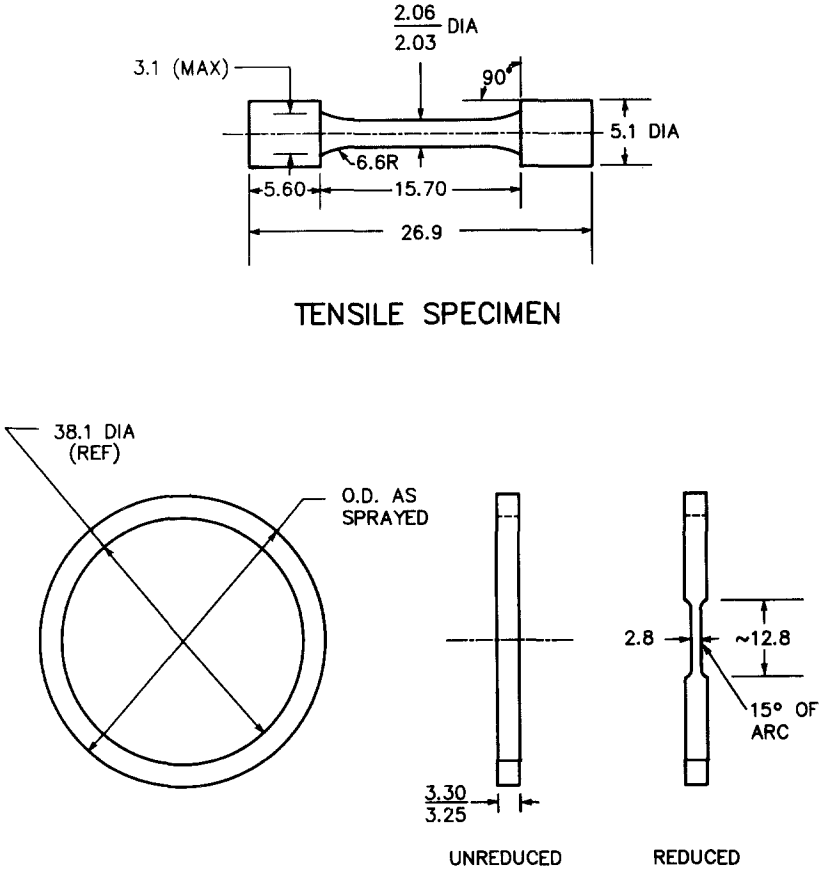

Figure 2 Drawings of tensile and ring specimens. Dimensions in millimetres.

3.2. Tensile test procedure

Cylindrical button-head specimens and ring tensile specimens were removed from the deposits described in Section 3.1 above. These were of two kinds. The button-head tensile specimens were taken from the thicker cylindrical deposit (~ 6.3 mm thick), with round cross-section blanks electrodischarge-machined from it. The test specimen dimensions are shown in Fig. 2.

The ring specimen is also shown in Fig. 2. Four different versions of the sample were evaluated. For one version, slices from a deposit with 0.12 mm wall thickness were cut to 3.3 mm wide and tested with the original as-sprayed rough outer surface. For a second version, the outer surface of the deposit was ground and polished to remove any surface-connected porosity, and then 3.3 mm wide slices were cut. For the other two versions, both the as-sprayed and the polished rings had two reduced sections each 2.8 mm in width and 15° of arc machined to make a minimum gauge length, as shown in Fig. 2. The reduced sections were centred on the junction of the D grips during testing. In all cases, the steel mandrel was removed chemically after machining in order to allow the mandrel to support the structure during machining.

All tensile testing was performed in an Instron testing machine using a crosshead speed of 0.051 cm min^{-1}. Tests at elevated temperature were performed in air in a nichrome-wound clam-shell type furnace. The button-head tensile specimens were held in conventional split-collet type grips. The ring specimens were held in pin-loaded D fixtures. A photograph of the fixtures and a ring specimen prior to test is shown in Fig. 3. The ring and fixture assembly was placed into an aligned load train and pulled to failure. The stress on the ring specimens was calculated by assuming that the load was carried equally at both sides at the D junction. Because the gauge length in such a specimen is, at best, ill-defined, the yield stress was estimated by drawing a 0.025 mm offset line parallel to the elastic loading line. Similarly, the measurement of ductility presented a problem. No attempt was made to estimate a reduction of area. Because the percentage of total elongation depends critically on the gauge length used in the test and increases rapidly with decreasing gauge length [14], and the gauge length in the ring tests was quite small (~ 0.3 mm) and ill-defined, elongation was measured as a total deflection.

3.3. Finite-element analysis

A finite-element analysis of the test specimen was performed to examine the strain distribution associated with the combined bending and tension at the test section. The specimen was modelled using two-dimensional plane stress theory; because of symmetry only one-quarter of the specimen was considered. The finite-element mesh, comprising seven- and eight-noded elements, is shown in Fig. 4. The D fixture is represented as a series of fixed nodes which correspond to the locations of nodes on the inner radius of the specimen. Coulomb friction was assumed between the D fixtures and the specimen. The material behaviour was taken to be elastic–plastic with isotropic hardening, and the stress–strain curve was obtained from the uniaxial data for IN-100 and

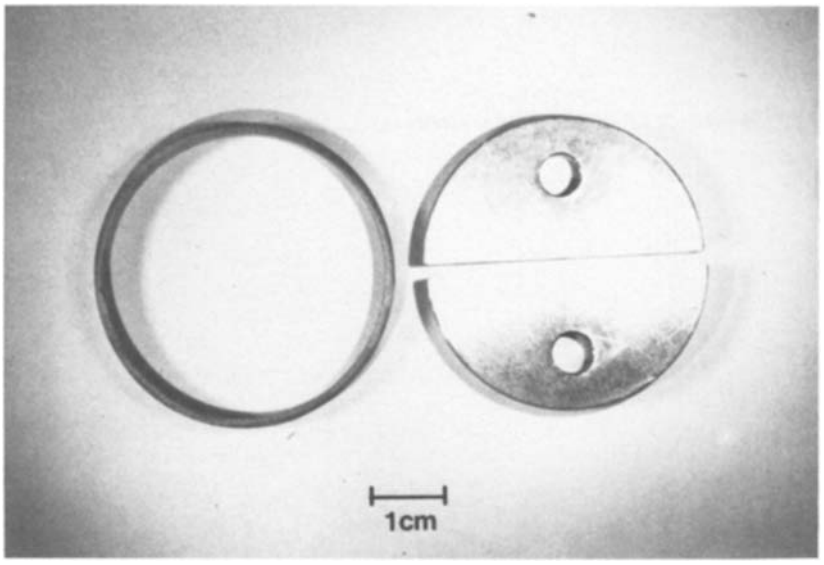

Figure 3 Photograph of D fixture and ring specimen prior to test.

simplified as bilinear for computational speed. The deformation of the specimen was analysed using the updated Lagrangian method in the ADINA finite-element program [15]. In this method, the equations of equilibrium are satisfied successively for small increments of motion of the D fixtures using an iterative method. Thus, the evolution of strain can be traced through its entire history. No failure criterion was applied, so the analysis was stopped at approximately the same displacement as was observed at failure of the test specimens.

4. Test results and discussion

Considering first the effect of the various treatments on the ring tensile properties of LPPD IN-100, these data are shown in Table I. The only significant effect observed was the somewhat lower strength for the as-deposited condition. This is attributed to the porous surface layer present on the LPPD deposit which is removed by subsequent polishing steps. Because of the presence of this surface layer in the as-sprayed and sprayed and reduced conditions, the specimen cross-sectional area was somewhat overestimated and the resulting strength was lower. Because of this, subsequent discussion of ring tensile properties will be restricted to the polished and polished/reduced condition.

The tensile properties of LPPD IN-100 cylindrical and ring specimens are shown in Table II as a function of test temperature. As indicated previously, because of a very small and ill-defined gauge length, the ring elongation is reported as total elongation. To represent the data in Table II in a form which allows the bar and ring tensile properties to be discussed and compared, a normalization scheme was used. Fig. 5 is a plot of the cylindrical tensile bar properties as a function of test temperature. These data were normalized with respect to the room-temperature properties and are shown as lines on Figs 6 to 9, 11 and 13. Superimposed on these lines are the normalized ring tensile properties from Table II. For clarity, separate plots are shown for the strength parameters (tensile and yield) and the elongation.

Considering first Figs 6 and 7, the points represent ring tensile strength data normalized with respect to the room-temperature *ring* tensile properties. There is remarkably good agreement between the ring and bar yield and tensile strength based on this normalization method. Although the polished/reduced normalized ring strengths appear higher, this is largely due to lower values of the room-temperature strength. An examination of values in Tables I and II show that the ring strengths are quite comparable.

When the ring tensile data are normalized with

TABLE I Ring tensile properties of LPPD IN-100 in various conditions*

Test temperature (°C)	Yield strength (MPa)				Ultimate tensile strength (MPa)				Elongation (mm)			
	AS	P	R	PR	AS	P	R	PR	AS	P	R	PR
25	937	985	892	885	1262	1416	1238	1272	1.88	2.46	1.42	1.65
	793	937	908	959	1164	1349	1207	1286	2.31	3.07	1.17	1.35
560	933	1003	898	954	1209	1296	1176	1258	0.71	1.50	1.30	1.47
	903	865	918	935	1214	1174	1116	1220	1.88	1.68	0.79	1.32
710	903	943	876	949	1037	1083	1014	1092	0.36	0.38	0.41	0.36
	943	978	940	892	1054	1101	1070	1057	0.38	0.36	0.36	0.64
860	631	642	640	674	678	674	693	700	0.18	0.08	0.15	0.08
	643	617	634	666	677	672	675	684	0.10	0.18	0.13	0.05
1010	239	248	264	243	274	274	290	272	0.31	0.15	0.15	0.15
	234	243	234	228	263	277	270	266	0.23	0.25	0.25	0.31

*AS = as-sprayed, P = polished, R = sprayed and reduced in gauge section, PR = polished and reduced.

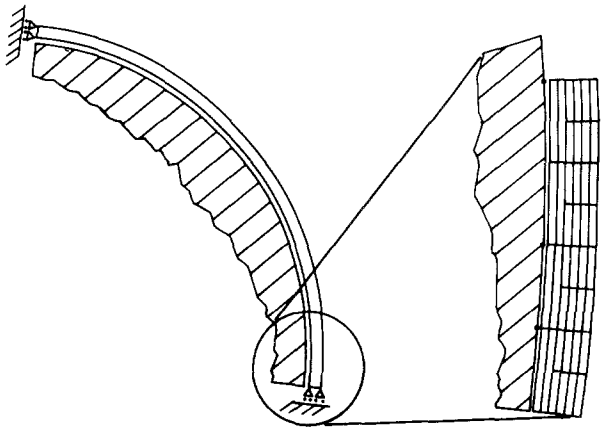

Figure 4 Finite-element model for ring test.

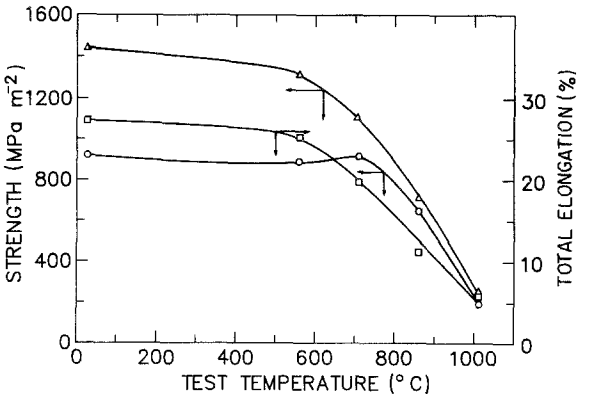

Figure 5 Uniaxial tensile properties using bar tensile specimens as a function of temperature for IN-100: (△) tensile strength, (○) yield strength, (□) elongation.

respect to the *bar* room temperature strength, the results are somewhat different (Figs 8 and 9). This mode of normalization allows a comparison of the ring and bar data, and shows that the yield strengths are roughly the same and the tensile strengths lower. Again, there is no systematic difference between the polished and polished/reduced conditions. The ring yield strengths are also probably lower than indicated; the very short gauge section undergoing deformation, together with the relatively insensitive measurement of the load–deflection curve, makes it likely that the 0.025 mm offset line used to define the ring yield strength actually overestimates it. At any rate, the ultimate ring tensile strength is about 8% lower than the bar strength at room temperature. The strength differences decrease with increasing temperature, and at 1010° C the ring strength is somewhat greater than the bar strength. Based on the subsequent discussions of the finite-element analysis and ductility comparison, this difference between bar and ring strength is not fully understood and probably represents an inherent difference between the two test methods.

The relatively good agreement between bar and ring tensile strength suggests that the bending contribution to the P/A strength is not as serious as in the case of composite rings [7, 9], and this indeed was found by the finite-element analysis. The distributions of the accumulated effective plastic strain predicted in the finite-element analysis for 25 and 710° C, using coefficients of friction of 0.0 and 0.1, are shown near the test section in Fig. 10. Each plot is for the approximate displacement at which failure of the specimen was observed during the experiments. In all cases, the strain is reasonably constant within at least $\frac{1}{2}$% across the test section. Because the tangent modulus is low at these high strains, similar plots of the equivalent stress show few features, indicating that the stress is practically constant. Because the stress and strain are a very close approximation to the uniaxial fields, the ring and bar yield and tensile strength values would be expected to be similar. As previously pointed out, Frankland and Roads [13] assumed a linear distribution in strain across the test section and solved for the axial load and the bending moment at the test section. They predicted that as the axial load is increased from zero, the bending moment increases from zero, through a peak, and then decreases toward zero. Thus, at high loads the linear distribution in strain becomes a constant distribution. This observation is consistent with the finite-element calculations.

Varying the friction coefficient influences the effective gauge section and, therefore, the strain to failure as indicated in Fig. 10. As the coefficient is increased the predicted strain increases, even though the displacements are identical in each case. Thus, the experimental results for the displacement to failure should be very dependent on the frictional boundary conditions. From test to test, the frictional conditions can be controlled fairly closely; however, the friction coefficient is known to increase with increasing temperature for some materials [16]. Because the effective gauge section is smaller than expected, the strain at failure cannot be calculated from the displacement at failure without further quantitative data regarding the frictional conditions.

TABLE II Tensile properties of LPPD IN-100

Test temperature (° C)	Yield strength (MPa)			Ultimate tensile strength (MPa)			% reduction of area		Total elongation			Uniform elongation	
	Bar	Ring average*		Bar	Ring average*		Bar	Ring	Bar (%)	Ring average* (mm)		Bar (%)	Ring average (PR)* (mm)
		P	PR		P	PR				P	PR		
25	920	961	922	1441	1383	1279	33.1	-	27.4	2.77	1.50	25.1	1.50
560	896	934	945	1309	1235	1239	30.7	-	25.3	1.59	1.40	21.5	1.40
710	919	961	921	1104	1092	1075	24.6	-	19.7	0.37	0.50	8.3	0.50
860	649	630	670	703	673	692	18.0	-	11.2	0.13	0.06	2.2	0.06
1010	196	246	236	247	276	269	11.1	-	6.0	0.23	0.23	2.2	0.23

*From Table I. P = polished, PR = polished and reduced.

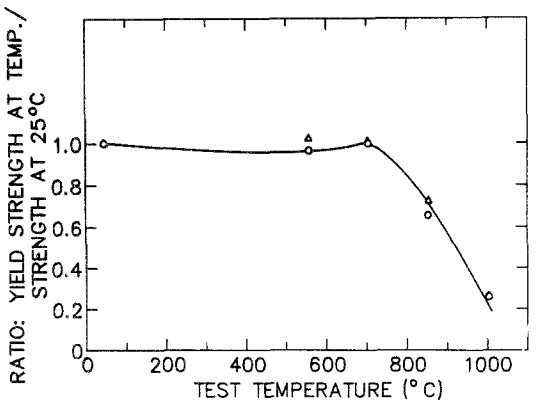

Figure 6 Yield strength normalized to room-temperature strength for the same type of specimen: (○) polished ring specimens, (△) polished and reduced ring specimens, (——) bar specimens.

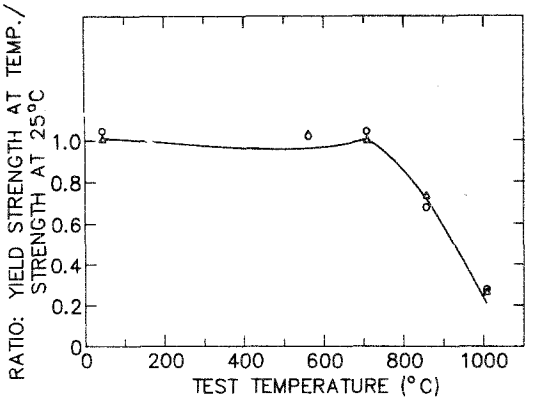

Figure 8 Yield strength normalized to room-temperature strength for bar specimens: (○) polished ring specimens, (△) polished and reduced ring specimens, (——) bar specimens.

Turning to the comparison of total elongation, the normalized bar and ring data are shown in Fig. 11. Normalization in this case can only be made with respect to the bar or ring because of the small and uncertain value of the gauge length. As may be seen from Fig. 11, both the polished and polished/reduced ring total elongation show what appears to be a ductility minimum while the bar data do not (based on limited test data). Similar ductility minima are seen for other superalloy systems and are often associated with dissolved oxygen. In this case dissolved oxygen is not sufficient to account for the discrepancy between bar and ring data, because the oxygen levels in the ring were only slightly higher (1000 p.p.m.) than the bar (800 p.p.m.). Typical ring tensile failures at 25 and 860° C are shown in Fig. 12 for polished specimens. Based on these ductility comparisons between polished and polished/reduced specimens, as well as the similarity of the strength values, it may be concluded that both the polished unreduced and reduced geometry may be used to evaluate ring tensile properties.

A possible explanation for the ductility differences indicated in Fig. 11 lies in the nature of the deformation process in the necking regime for the bar and ring cases. As may be seen in Table II, the uniform elongation to ultimate load decreases with respect to temperature and contributes less to the total elongation for the case of the bar, while the uniform and total elongations for the ring are identical, i.e. necking does not occur. This was also evident from an examination of the ring fractures. As indicated in Section 3.2., no attempt was made to measure the ring reduction of area (RA) after fracture, but nothing approaching the value of 30% RA measured for the bar was observed in the ring. It is likely that in restricting the deformation of the ring specimen to the small volume at the D junction inhibits necking deformation. Whatever the reason, localized deformation does not occur for LPPD IN-100, and if the normalized uniform elongation of the bar is compared to that of the rings, the comparison is very good, as may be seen in Fig. 13.

It should be noted that in other ring tensile tests performed in this laboratory on quite ductile materials, local deformation has been observed with both the ring width and thickness showing a contraction. Whether or not local deformation occurs in the ring test is a complex problem, depending on the friction coefficient and the deformation behaviour of the material being evaluated.

The lack of any significant necking strain in the present ring tests (which may be seen in the photographs in Fig. 12) may account for the somewhat lower ring tensile strength as compared to the bar strength (see Table II and Fig. 9). Because necking is prevented, the ring may fail prematurely at a some-

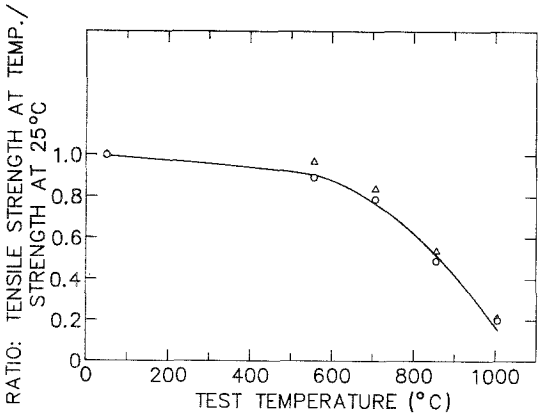

Figure 7 Tensile strength normalized to room-temperature strength for the same type of specimen: (○) polished ring specimens, (△) polished and reduced ring specimens, (——) bar specimens.

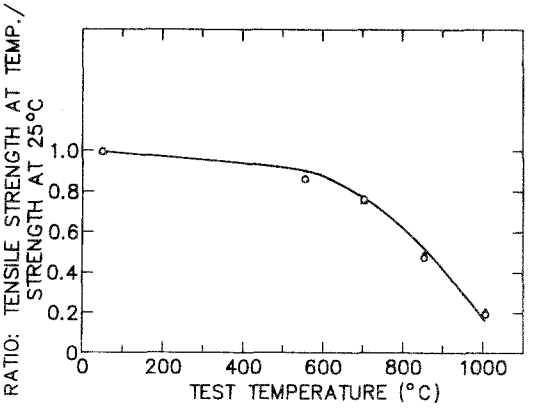

Figure 9 Tensile strength normalized to room-temperature strength for bar specimens: (○) polished ring specimens, (△) polished and reduced ring specimens, (——) bar specimens.

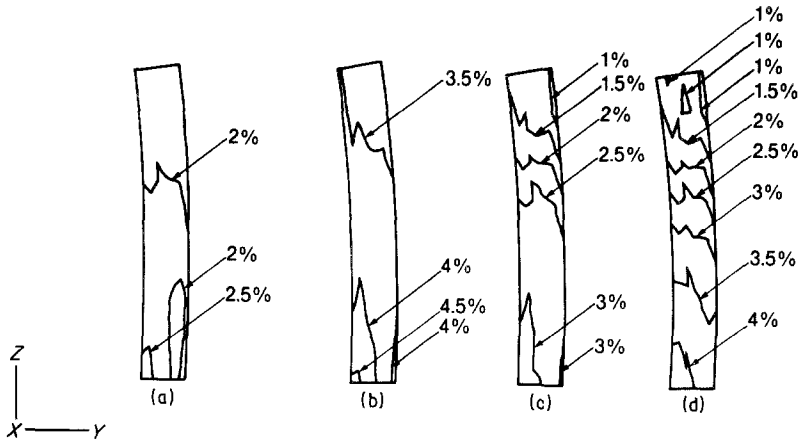

Figure 10 Contours of equivalent plastic strain for (a) $\mu = 0.0$, $T = 25°C$ at 1.52 mm displacement; (b) $\mu = 0.1$, $T = 25°C$ at 1.52 mm displacement; (c) $\mu = 0.0$, $T = 710°C$ at 0.51 mm displacement; (d) $\mu = 0.1$, $T = 710°C$ at 0.51 mm displacement.

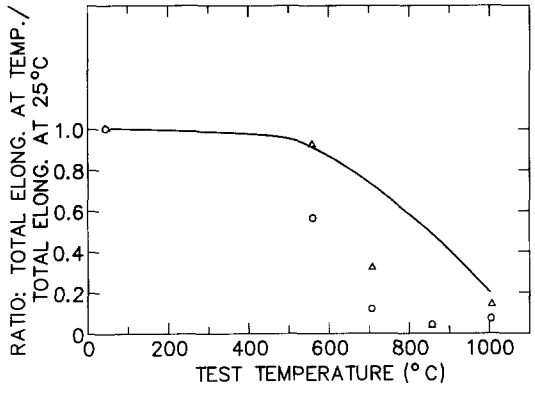

Figure 11 Total elongation normalized to room-temperature elongation for the same type of specimen: (○) polished ring specimens, (△) polished and reduced ring specimens, (——) bar specimens.

what lower stress than an unrestrained tensile bar. However, because of the similarity of the two uniform elongations, this cannot be a large effect, and indeed the two strengths differ by only 8%, as indicated previously.

Finally, some general observations may be made regarding the ring tensile test. The test has been used extensively in this laboratory for the past year to evaluate LPPD process variations; and as the data presented in this paper have shown, the test can accurately measure the tensile properties and provide guidance in ductility trends. In using this test in the manner described herein, several precautions must be observed. Most importantly, if the elongation is very low (particularly at high strength levels and/or low temperatures), the ring tensile values are suspect. Analysis and experience indicates that in this case the bending component of the stress at the D junctions can significantly lower the measured P/A stress. In some cases this low ductility is not necessarily an intrinsic property of the LPPD material, but is due to mandrel/deposit reactions at the internal diameter of the ring, leading to a compositional gradient through the ring wall thickness.

Other precautions to be observed are those inherent in most test methods, such as adequate specimen alignment. The D fixtures should fit snugly about the ring internal diameter, and the gap should not exceed ~0.30 mm. It has been found useful to have several sets of D fixtures available to accommodate slightly differing ring sizes.

5. Conclusions

Based on the data presented in this paper, the following conclusions may be drawn:

1. The ring tensile test as described in this paper is an adequate test to rapidly evaluate thin-walled

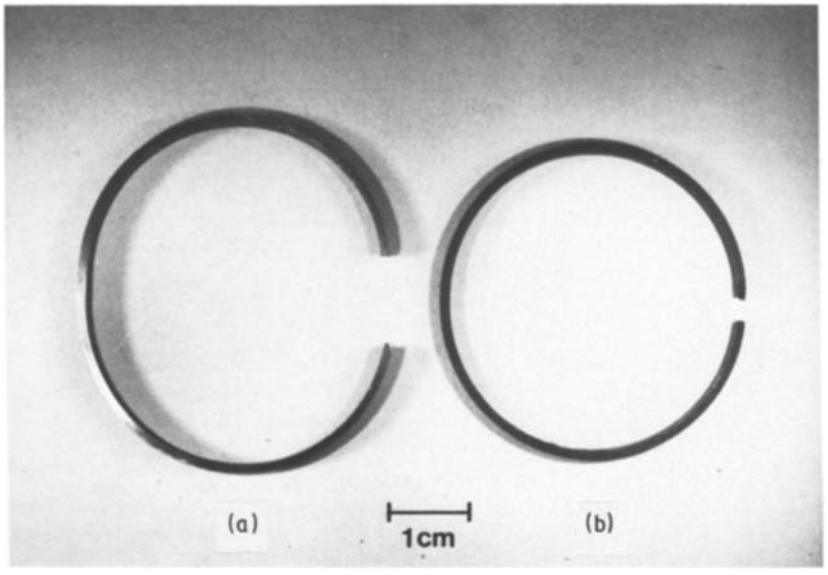

Figure 12 Fractured IN-100 ring specimens: (a) $T = 25°C$, (b) $T = 860°C$.

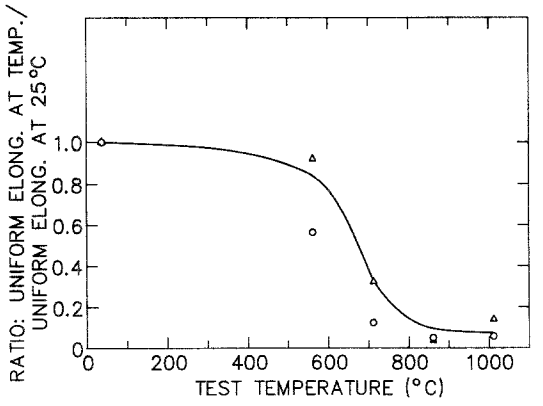

Figure 13 Uniform elongation normalized to room-temperature elongation for the same type of specimen: (○) polished ring specimens, (△) polished and reduced ring specimens, (——) bar specimens.

plasma-sprayed structures. As long as some ductility is present, the strength values obtained from such a test are at most 8% lower than the uniaxial tensile strength. A ring test with either a reduced or unreduced gauge section may be used.

2. Finite-element analysis indicates that the stress and strain distributions for large displacements are a close approximation to those for the uniaxial distribution.

3. Frictional boundary conditions play an important role in determining the magnitude of the strain at failure. Further information would be necessary to accurately describe strain at failure for the ring test. In addition, because of the geometry of the ring tensile test, necking generally will not occur and a reduction of area similar to that measured in a uniaxial tensile test is not usually obtained.

Acknowledgements

We would like to acknowledge the contribution of J. Resue in producing the deposits, C. Canestraro in obtaining the tensile data, and E. Sauter for metallographic preparation.

References

1. T. A. ROSEBERRY and F. W. BOULGER, "A Plasma Flame Spray Handbook", Report No. MT-043, Naval Sea Systems Command, Dept. of the Navy (1977).
2. E. MUEHLBERGER, in Proceedings of 7th International Thermal Spray Conference, London, 1973, p. 245.
3. M. R. JACKSON, J. R. RAIRDEN, J. S. SMITH and R. W. SMITH, *J. Metals* **33** (1981) 23.
4. J. R. RAIRDEN, in Proceedings of 9th International Thermal Spray Conference, The Hague, 1980, p. 329.
5. P. A. SIEMERS, M. R. JACKSON, R. L. MEHAN and J. R. RAIRDEN, *Ceram. Eng. Sci. Proc.* **6** (1985) 896.
6. A. M. SHIBLEY, H. L. PERITT and M. EIG, "A Survey of Filament Winding: Materials, Design Criteria, Military Applications", Plastec Report 10 (Plastics Technical Evaluation Center, Picatinny Arsenal, Dover, New Jersey, 1962).
7. C. E. KNIGHT, ASTM STP 617 (American Society for Testing and Materials, Philadelphia, 1977) p. 201.
8. "Standard Test Method for Apparent Tensile Strength of Ring or Tubular Plastics and Reinforced Plastics by Split Disk Method", ASTM Designation D2290-76. 1983 Annual Book of ASTM Standards, Vol. 15.03 (American Society for Testing and Materials, Philadelphia).
9. N. F. DOW, B. W. ROSEN, L. S. SHU and C. H. ZWEBEN, "Design Criteria and Concepts for Fibrous Composite Structures", NASA-CR-66515 (1967).
10. M. VEMURA and M. MURATA, *J. Soc. Mater. Sci. Jpn* **27** (1978) 81.
11. V. F. KRASHCHENKO and A. E. GURARII, *Ind. Lab.* **51** (1985) 1044.
12. V. A. KOLESNICKENKO and R. S. YUSUPOV, *Fiz. Khim. Obrab. Mater.* **3** (1978) 148.
13. J. M. FRANKLAND and R. E. ROADS, *J. Aerospace Sci.* **21** (1954) 449.
14. J. R. LOW, in "Properties of Metals in Materials Engineering" (American Society for Metals, Metals Park, Ohio, 1949) pp. 17–59.
15. "ADINA - A Finite Element Program For Automatic Dynamic Incremental Nonlinear Analysis", Report AE 84-1 (ADINA Engineering, Watertown, Massachusetts and Vasterus, Sweden).
16. D. HOFFMAN and G. SACKS, "Introduction to the Theory of Plasticity for Engineers" (McGraw-Hill, New York, 1953) p. 64.

Received 26 February
and accepted 29 April 1987